Chemical Engineering Journal 166 (2011) 348–357

Contents lists available at ScienceDirect

Chemical Engineering Journal

journal homepage: www.elsevier.com/locate/cej

Comparison studies of xylene isomerization and disproportionation reactions between SSZ-33, TNU-9, mordenite and ZSM-5 zeolite catalysts

Nasiru M. Tukur[a], Sulaiman Al-Khattaf[b,*]

[a] SABIC E&PM, P. O. Box 11425, Jubail Industrial City 31961, Saudi Arabia
[b] Center of Excellence in Petroleum Refining and Petrochemicals (CoRE-PRP), King Fahd University of Petroleum & Minerals, Dhahran 31261, Saudi Arabia

ARTICLE INFO

Article history:
Received 24 July 2010
Received in revised form 20 October 2010
Accepted 1 November 2010

Keywords:
Xylene reactions
ZSM-5
Mordenite
SSZ-33
TNU-9
Isomerization
Disproportionation

ABSTRACT

m-Xylene isomerization and disproportionation kinetics have been studied over four zeolite catalysts (ZSM-5, mordenite, SSZ-33 and TNU-9) in a riser simulator reactor over the temperature range of 300–400 °C. The effect of reaction conditions on *m*-xylene conversion, *p*-xylene/*o*-xylene (P/O) ratios, ratio of isomerization to disproportionation (I/D) products were investigated with the view of comparing the respective performances of the catalysts. Kinetic parameters for the disappearance of *m*-xylene were determined using catalyst activity decay function based on time-on-stream (TOS). The experimental results show that SSZ-33, TNU-9 and mordenite gave higher *m*-xylene conversion compared to ZSM-5. Both *m*-xylene P/O and I/D ratios over the catalysts were found to be in the order: ZSM-5 > TNU-9 > SSZ-33 > mordenite. Apparent activation energy for *m*-xylene disproportionation reaction was found to decrease in the order: $E_{ZSM-5} > E_{TNU-9} > E_{mordenite} > E_{SSZ-33}$. The riser simulator and the modeling procedures employed have proved to be very effective as tools in investigating fluidized bed reaction kinetics.

1. Introduction

The demand for *p*-xylene as a starting raw material for the manufacture of terephthalic acid (PTA) has increased tremendously over the past years. Nearly all *p*-xylene recovered from petroleum in the US is consumed in the manufacture of PTA, which is used in the production of polyester fibers, resin, and film. Some *p*-xylene is used as a solvent and in the manufacture of di-paraxylene and herbicides.

p-Xylene has the largest commercial market as compared to its isomers, meta-xylene (*m*-xylene) and ortho-xylene (*o*-xylene). With increasing demand of *p*-xylene, selective production of *p*-xylene by *m*-xylene isomerization using zeolite catalyst has gained considerable interest over the years and much attention has been focused on ZSM-5 zeolite as catalyst due to its high activity and shape selectivity as previously stated [1,2].

Xylene transformation reactions over zeolite catalysts are complex. Besides, isomerization and disproportionation, dealkylation and transalkylation reactions might also be present. The complexity of the transformation reactions and the interplay of diffusion and chemical reactions have often led to different reaction pathways.

Two reaction schemes have been used in the literature to model xylene transformation reactions. The first one is the triangle reaction path [3–5] among others, where *p*-xylene could be converted directly into *o*-xylene. This is explained by the fast movement of the para isomer inside the porous catalyst which might cause an apparent 1,3 shift of the methyl group in the benzene ring as shown by Young et al. [6]. The second scheme on the other hand, assumes that the reaction proceeds via 1,2-methyl shift only where one of the methyl groups in *m*-xylene might shift to the adjacent positions through a series of consecutive, reversible 1,2-methyl shift mechanism and become *o*-xylene or *p*-xylene [7–10].

Shape selective conversion of xylenes over ZSM-5 has been investigated in detail by several workers [6,7,11]. Chang et al. [5] used a pulse micro reactor-chromatograph technique to study the xylene isomerization reaction over HZSM-5 zeolite catalyst. Their reported activation energies indicated that the transformation of *m*-xylene to *o*- or *p*-xylene, *o*-xylene to *m*- or *p*-xylene, and *p*-xylene to toluene are controlled by reaction, and the conversion of *p*-xylene to *m*- or *o*-xylene is in the transition regime of diffusion and reaction. Ma and Savage [12] also studied xylene isomerization over ZSM-5 to observe the effects of site modification on the reaction. The kinetic, diffusion, and adsorption parameters they determined were generally in agreement with literature.

Iliyas and Al-Khattaf [13] reported a detailed kinetic and selectivity study of xylene transformation using Y-zeolite in a riser simulator that mimics the operation of a fluidized bed reactor.

* Corresponding author. Tel.: +966 3 860 1344; fax: +966 3 860 4509.
E-mail address: skhattaf@kfupm.edu.sa (S. Al-Khattaf).

1385-8947/$ – see front matter © 2010 Elsevier B.V. All rights reserved.
doi:10.1016/j.cej.2010.11.004

Nomenclature

C_i	concentration of specie i in the riser simulator (mole/m^3)
CL	confidence limit
E_i	apparent activation energy of ith reaction (kJ/mol)
k	apparent kinetic rate constant (m^3/kgcat s). $= k'_0 \exp[-E_R/R(1/T - 1/T_0)]$
k'_0	pre-exponential factor in Arrhenius equation defined at an average temperature [m^3/kgcat s], units based on first order reaction
MW_i	molecular weight of specie i
r	correlation coefficient
R	universal gas constant (kJ/kmol K)
t	reaction time (s)
T	reaction temperature (K)
T_0	average temperature of the experiment
V	volume of the riser (45 cm^3)
W_c	mass of the catalysts (0.81 gcat)
W_{hc}	total mass of hydrocarbons injected in the riser (0.162 g)
y_i	mass fraction of ith component (wt%)

Greek letter

α	apparent deactivation constant (s^{-1}) (TOS model)

Similarly, xylene reactions and diffusions in ZSM-5 zeolite based catalyst were investigated and modeled over a fluidized bed reactor by Al-Khattaf [14]. The author modeled the kinetic reactions using time-on-stream model and determined the intrinsic kinetic parameters for both isomerization and disproportionation reactions. The results also showed that *m*-xylene effectiveness factor was less than 0.1 indicating a high diffusion obstacle inside ZSM-5 zeolite. While *o*-xylene had effectiveness factor in the range of 0.35–0.45, *p*-xylene effectiveness factor was found to be close to unity indicating no diffusion limitation.

Although abundant literatures have been published and numerous patents filed on xylene transformation over different zeolites, however, in most instances, fixed-bed reactor has been utilized for the reaction and only of recent was fluidized bed reactor considered. In view of this, it is of interest to extend xylene transformation in the riser simulator to other medium and large pore zeolites, such as TNU-9, mordenite and SSZ-33. This will afford the opportunity to study the reaction over these zeolites under short reaction time of the riser simulator. However, it should be noted that recently that Žilková et al. [15] reported studies of toluene disproportionation and alkylation over SSZ-33. Also, Llopis et al. [16] reported xylene isomerization and aromatic alkylation in zeolites NU-87, SSZ-33, β, and ZSM-5 carried out in a fixed-bed reactor.

Zeolite SSZ-33 (CON topology) possesses a channel system of intersecting 12-ring and 10-ring pores; it is the first synthetic zeolite having 4-4 = 1 SBU (secondary building unit) in the structure [17]. TNU-9 represents a new three-dimensional zeolites with 10 ring channel systems, being rather similar to the industrially most frequently employed ZSM-5. The size of the channels of TNU-9 is 0.52 nm × 0.60 nm and 0.51 nm × 0.55 nm, thus a slightly larger zeolite compared with ZSM-5 as indicated by Cejka et al. [18].

In this work, the catalytic activity of TNU-9 zeolite possessing 10-10-10-ring system is compared with SSZ-33 (12-12-10), ZSM-5 (10-10-10) and mordenite (12-8) in xylene isomerization and disproportionation reactions. Although there are several studies on xylene transformation reactions over ZSM-5 and mordenite based catalysts, very few (if any) are reported over SSZ-33 and TNU-9 based catalysts. Furthermore, most of the reported studies are related to catalyst development and reaction mechanisms only with no modeling.

In addition, the current study will investigate the effect of reaction conditions on *m*-xylene conversion, *p*-xylene/*o*-xylene (P/O) ratios, ratio of isomerization to disproportionation (I/D) products over the four zeolites with the view of comparing their respective performances. Kinetic parameters for the disappearance of *m*-xylene via isomerization and disproportionation pathways will be determined using the catalyst activity decay function based on time-on-stream (TOS). To our knowledge, the kinetic modeling of xylene isomerization and disproportionation reactions carried in a fluidized bed reactor over TNU-9, SSZ-33 and mordenite based catalysts have not been reported in the open literature.

2. Experimental procedure

2.1. Preparation of catalysts

The uncalcined proton form of mordenite (H-mordenite) zeolite (HSZ-690HOA) used in this work was obtained from Tosoh Chemicals, Japan. The mordenite has silica to alumina ratio of 240. An alumina binder (Cataloid AP-3) contains 75.4 wt% alumina, 3.4% acetic acid and water as a balance obtained from CCIC Japan. The alumina binder was dispersed in water and stirred for 30 min to produce thick slurry. The zeolite powder was then mixed with alumina slurry to produce a thick paste. The composition of the zeolite based catalyst in weight ratio is as follows: Mordenite:AP-3 (2:1).

The uncalcined proton form of ZSM-5 (CT-405) used in this study was obtained from CATAL, UK. The ZSM-5 has silica to alumina ratio of 30. Similar procedure used for the preparation of the mordenite based catalyst used in this study was also followed for the preparation of the ZSM-5 based catalyst. The composition of the ZSM-5 zeolite based catalyst in weight ratio is as follows: ZSM-5:AP-3 (2:1).

Zeolite SSZ-33 and TNU-9 and their characterization data (SEM, FTIR) used in this study were obtained from J. Heyrovsky Institute of Physical Chemistry, Academy of Science of the Czech Republic, Prague, Czech Republic. Alumina was added to these zeolites (SSZ-33 and TNU-9) adopting the same procedure used for mordenite and ZSM-5 based catalyst.

2.2. Characterization of catalysts

Surface areas were obtained from N_2 physical adsorption isotherms by applying BET method with Quanta chrome AUTOSORB-1 (model # ASI-CT-8). The samples were preheated at 373 K for 3 h in flowing N_2. Type and concentration of acid sites in all zeolites were determined by adsorption of pyridine as probe molecules followed by FTIR spectroscopy (Nicolet 6700 FTIR) using the self-supported wafers technique. Prior to adsorption, self-supporting zeolite wafers were activated in situ by evacuation at temperature 450 °C over night. Adsorption of pyridine proceeded at 150 °C for 20 min at partial pressure 5 Torr.

The concentrations of Bronsted and Lewis acid sites were calculated from the integral intensities of individual bands characteristic of pyridine on Bronsted acid sites at 1550 cm^{-1} and band of pyridine on Lewis acid sites at 1455 cm^{-1} and molar absorption coefficient [19] of $\varepsilon(B) = 1.67 \pm 0.1$ cm μmol^{-1} and $\varepsilon(L) = 2.22 \pm 0.1$ cm μmol^{-1}, respectively. The infrared spectra of absorbed pyridine on SSZ-33 were recently discussed in detail by Gil et al. [20]. The characteristics of all samples are given in Table 1.

X-ray powder patterns of all zeolites under study exhibited good crystallinity and characteristic diffraction lines (not shown here). The shape and size of all zeolites were determined by scanning electron microscopy (Jeol, JSM-5500LV). Fig. 1 shows typical SEM

Table 1
Characteristics of samples used in this work.

Sample code	Si/Al	Lewis sites (mmol/g)	Bronsted sites (mmol/g)	Lewis sites (%)	Bronsted sites (%)	BET (m^2/g)
Parent-ZSM-5	30.0	0.13	0.24	35	65	
F.C-ZSM-5	20.3	0.28	0.21	57	43	304
Parent-TNU-9	21.9	0.15	0.43	26	74	
F.C-TNU-9	19.3	0.25	0.33	43	57	330
Parent-MOR	180	<0.002	0.03	4	96	
F.C-MOR	135.9	0.12	0.03	80	20	441
Parent-SSZ-33	18	0.43	0.30	59	41	
F.C-SSZ-33	13.6	0.48	0.18	72	28	448
AP-3		0.64	0	100	0	280

F.C.: final catalyst.

images of zeolites SSZ-33 and TNU-9. The SEM images evidence the absence of impurities including an amorphous one. The crystal sizes of all zeolites used in this present study were between 0.3 and 1 μm. Table 1 provides the quantitative evaluation of FTIR spectra of parent zeolites and final catalysts. It was observed that addition of alumina binder led to the decrease in Si/Al ratio for all catalysts and to a simultaneous increase in the concentration of Lewis acids sites.

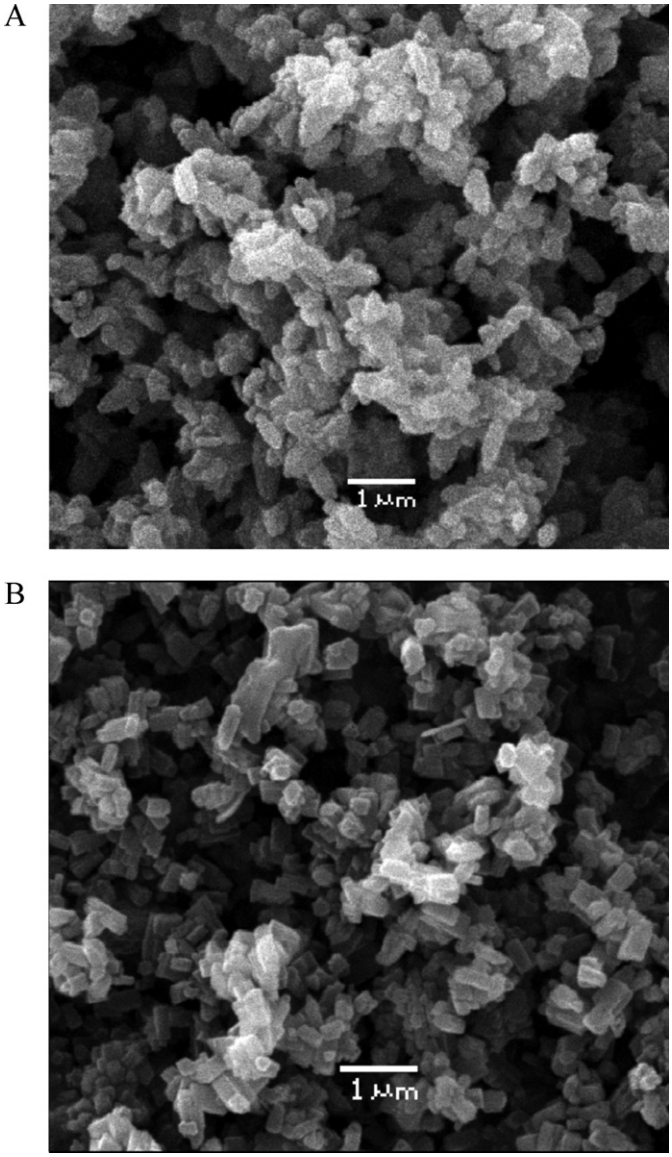

Fig. 1. SEM images of SSZ-33 (A) and TNU-9 (B).

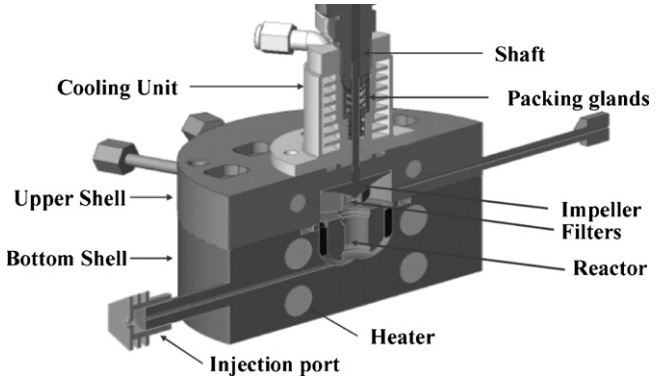

Fig. 2. Schematic diagram of the riser simulator.

2.3. Reaction procedure

Xylene isomerization and disproportionation reactions were carried out in the riser simulator (see Fig. 2). This reactor is bench scale equipment with internal recycle unit invented by de Lasa [21]. A detailed description of various riser simulator components, sequence of injection and sampling can be found in Kraemer [22]. Catalytic experiments were carried out in the riser simulator for residence times of 5, 10, 15 and 20 s at temperatures of 300, 350 and 400 °C. About 800 mg of the catalyst was weighed and loaded into the riser simulator basket. The system was then sealed and tested for any pressure leaks by monitoring the pressure changes in the system. Furthermore, the reactor was heated to the desired reaction temperature. The vacuum box was also heated to ~250 °C and evacuated to a pressure of ~0.5 psi to prevent any condensation of hydrocarbons inside the box. The heating of the riser simulator was conducted under continuous flow of inert gas (Ar), and it usually takes a few hours until thermal equilibrium is finally attained. Meanwhile, before the initial experimental run, the catalyst was activated for 15 min at 620 °C in a stream of Ar. The temperature controller was set to the desired reaction temperature, and in the same manner, the timer was adjusted to the desired reaction time. At this point, the GC is started and set to the desired conditions.

Once the reactor and the gas chromatograph have reached the desired operating conditions, 0.162 g of the feedstock was injected directly into the reactor via a loaded syringe. After the reaction, the four-port valve opens immediately, ensuring that the reaction was terminated and the entire product stream was sent on-line to analytical equipment via a preheated vacuum box chamber. The products were analyzed in an Agilent 6890N gas chromatograph with a flame ionization detector and a capillary column INNOWAX, 60-m cross-linked methyl silicone with an internal diameter of 0.32 mm. During the course of the investigation, a number of runs were repeated to check for reproducibility in the experimental results, which were found to be excellent. Typical errors were in the range of ±2%.

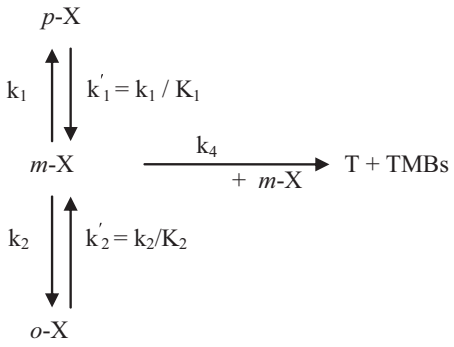

Scheme 1.

3. Kinetic model development

The experimental results were modeled using steady state approximations with catalyst decay to be function of time on stream. The kinetic model representing xylene transformation reactions is based on isomerization and disproportionation reactions only. As shown in the reaction network in Scheme 1, the reactions involved are: (i) isomerization of *m*-xylene to *p*-xylene, (ii) isomerization of *m*-xylene to *o*-xylene, and (iii) disproportionation of *m*-xylene to give trimethylbenzenes (TMBs) and toluene (T).

Based on the assumption that isomerization and disproportionation proceed via monomolecular and bimolecular mechanism, respectively, the isomerization reaction was described by a first order rate equation and the disproportionation by second order rate equation. Similar assumptions were used in related studies [2,23]. Minor reactions are not included in the model, like transalkylation, dealkylation, to give benzene and tetramethylbenzenes (TeMBs) and gases. In this scheme, one of the methyl groups in *m*-xylene might shift to the adjacent positions through a series of consecutive, reversible 1,2-methyl shift mechanism and become *o*-xylene or *p*-xylene. However, direct conversion of *p*-xylene to *o*-xylene is not possible.

The following first order differential equations are the model equations that were derived based on Scheme 1.

Rate of disappearance of *m*-xylene

$$\frac{dy_{m-x}}{dt} = -\left\{(k_1 y_{m-x} - k'_1 y_{p-x})\frac{W_c}{V} + (k_2 y_{m-x} - k'_2 y_{o-x})\frac{W_c}{V} + 2k_4 y_{m-x}^2 \left(\frac{W_c W_{hc}}{V^2 MW_{m-x}}\right)\right\} \exp(-\alpha t) \quad (1)$$

Rate of formation of toluene

$$\frac{dy_{tol}}{dt} = k_4 y_{m-x}^2 \left(\frac{W_c W_{hc} MW_{tol}}{V^2 MW_{m-x}^2}\right) \exp(-\alpha t) \quad (2)$$

Rate of formation of *p*-xylene

$$\frac{dy_{p-x}}{dt} = (k_1 y_{m-x} - k'_1 y_{m-x})\frac{W_c}{V} \exp(-\alpha t) \quad (3)$$

Rate of formation of *o*-xylene

$$\frac{dy_{o-x}}{dt} = (k_2 y_{m-x} - k'_2 y_{m-x})\frac{W_c}{V} \exp(-\alpha t) \quad (4)$$

where y_x is the mass fraction of species x in the riser simulator, MWx is the molecular weight of specie x in the system, V is the volume of the riser (45 cm^3), W_{hc} is the weight of feedstock injected into the reactor (0.162 g), W_c is the mass of the catalyst (0.81 g of catalyst), t is the time (s), α is deactivation constant; and k, rate constant (cm^3/gcat s).

It should be noted that the following additional assumptions were made in deriving the reaction network:

1. A reversible reaction path is assumed for isomerization, while irreversible reaction is presumed for disproportionation.
2. Trimethylbenzenes are entirely the results of the disproportionation reaction. [The disproportionation reaction involves the formation of 1 mole of toluene and 1 mole of trimethylbenzenes from 2 moles of *m*-xylene.]
3. The model assumes catalytic reactions only and neglects thermal conversion. This hypothesis of a negligible contribution from thermal reactions has been fully justified.
4. A single deactivation function defined for all the reactions taking place.
5. Dealkylation reaction is inconsequential due to the minor amounts of gases in the reaction system.
6. The reactor operates under isothermal conditions, justified by the negligible temperature change observed during the reactions.

The influence of temperature on the model parameters can be accounted for, through the following Arrhenius equation:

$$k_i = k_{0_i} \exp\left(\frac{-E_i}{R}\left[\frac{1}{T} - \frac{1}{T_0}\right]\right) \quad (5)$$

where T_0 is the average reaction temperature introduced for to reduce parameter interaction.

In order to ensure thermodynamic consistency at equilibrium, the rate constants for *m*- to *p*-xylene, and *m*- to *o*-xylene reactions in the above equations are expressed as follows by Gendy [24]:

$$K_1 = \frac{k_1}{k'_1} \quad (6)$$

$$K_2 = \frac{k_2}{k'_2} \quad (7)$$

where $K_1 = (C_p/C_m)_{eq}$ and $K_2 = (C_o/C_m)_{eq}$ are temperature-dependent equilibrium constants for both reactions, respectively. However, an average value can be computed for both constants, because the thermodynamic equilibrium concentrations of the xylenes remain fairly constant within the temperature range of this work. The xylene equilibrium concentrations are obtained from the published work of Stull et al. [25].

4. Results and discussion

4.1. m-Xylene isomerization and disproportionation reactions over 4 zeolites catalyst

The product distribution for the isomerization and disproportionation reactions of *m*-xylene feedstock over the ZSM-5 zeolite catalyst is presented in Table 2. Tables 3–5 are the product distributions over Mordenite, SSZ-33 and TNU-9, respectively. As shown in these tables, the major reaction products are: the other two xylene isomers (*p*-xylene and *o*-xylene), trimethylbenzenes and toluene. Traces of benzene and tetramethylbenzenes were also observed in the reaction mixtures, however, the yields of these products were very low. It can be seen from these tables that the yield of the various products increases with both reaction time and temperature.

Disproportionation reaction requires two molecules of xylene reactants with bulky transition state intermediates. As a result, disproportionation is significant on medium and large pore zeolites such as Mordenite, SSZ-33 and TNU-9 that can accommodate these intermediates. However, in ZSM-5 zeolites with a smaller pore size, it is difficult to form the intermediates of disproportionation pathway (restricted transition state selectivity). This explains

Table 2
Product distribution (wt%) at various reaction conditions for *m*-xylene isomerization and disproportionation reactions over ZSM-5 catalyst.

Temp (°C)/time (s)	Conversion (%)	*m*-Xylene	*p*-Xylene	*o*-Xylene	Toluene	TMBs
300						
5	13.13	86.87	6.60	3.40	2.21	0.86
10	19.36	80.64	9.15	4.32	2.29	0.79
15	27.33	72.67	13.91	7.33	3.95	1.89
20	28.87	71.13	15.52	7.46	4.45	1.34
350						
5	19.26	80.74	9.09	4.59	3.23	1.22
10	27.34	72.66	13.29	6.88	4.26	1.77
15	34.61	65.39	15.92	9.33	5.65	2.57
20	36.85	63.15	17.03	10.40	6.22	2.86
400						
5	24.73	75.27	10.03	6.40	4.84	2.97
10	34.37	65.63	13.97	9.25	6.49	3.96
15	41.93	58.07	15.84	11.52	8.35	5.23
20	43.73	56.27	16.60	12.46	8.64	5.06

Table 3
Product distribution (wt%) at various reaction conditions for *m*-xylene isomerization and disproportionation reactions over mordenite.

Temp (°C)/time (s)	Conversion (%)	*m*-Xylene	*p*-Xylene	*o*-Xylene	Toluene	TMBs
300						
5	27.99	72.01	4.97	5.17	7.64	7.10
10	38.55	61.45	7.06	7.29	10.64	10.27
15	45.65	54.35	8.52	8.72	13.50	13.15
20	51.89	48.11	9.06	9.16	15.56	15.20
350						
5	31.88	68.12	4.72	4.60	9.81	10.27
10	47.68	52.32	6.75	6.49	14.63	15.47
15	54.70	45.30	7.92	7.53	16.89	17.61
20	60.12	39.88	8.60	8.13	18.54	19.23
400						
5	34.71	65.29	4.75	4.65	10.20	11.23
10	49.45	50.55	6.85	6.60	14.95	16.60
15	56.09	43.91	7.68	7.38	16.89	18.90
20	62.80	37.20	8.50	8.18	18.67	21.35

Table 4
Product distribution (wt%) at various reaction conditions for *m*-xylene isomerization and disproportionation reactions over SSZ-33.

Temp (°C)/time (s)	Conversion (%)	*m*-Xylene	*p*-Xylene	*o*-Xylene	Toluene	TMBs
300						
5	30.14	69.86	5.34	4.07	9.38	8.83
10	44.03	55.97	7.61	5.91	13.44	13.18
15	52.66	47.34	8.71	6.94	16.07	15.58
20	56.91	43.09	9.31	7.42	17.52	17.34
350						
5	33.44	66.56	5.42	4.55	10.04	9.47
10	47.15	52.85	7.27	6.15	14.95	12.63
15	56.40	43.60	8.48	7.30	17.51	15.68
20	61.00	39.00	8.70	7.55	19.26	16.54
400						
5	37.25	62.75	5.67	4.94	11.38	9.50
10	50.65	49.35	7.50	6.63	16.00	12.99
15	57.71	42.29	8.10	7.32	18.62	14.31
20	62.80	37.20	8.63	7.84	20.03	16.60

Table 5
Product distribution (wt%) at various reaction conditions for *m*-xylene isomerization and disproportionation reactions over TNU-9.

Temp (°C)/time (s)	Conversion (%)	*m*-Xylene	*p*-Xylene	*o*-Xylene	Toluene	TMBs
300						
5	28.20	71.80	4.59	4.09	9.46	7.68
10	43.84	56.16	7.10	6.39	14.08	12.68
15	52.50	47.50	8.06	7.31	16.36	15.44
20	58.43	41.57	8.99	8.13	18.15	17.83
350						
5	32.69	67.31	6.11	4.77	10.04	8.15
10	48.14	51.86	8.65	6.91	14.97	11.99
15	55.41	44.59	9.90	8.01	16.72	14.78
20	61.04	38.96	9.95	8.48	19.14	15.71
400						
5	36.49	63.51	6.39	5.19	11.48	8.50
10	48.79	51.21	8.07	6.72	15.72	11.04
15	56.11	43.89	8.75	7.55	18.45	12.72
20	62.75	37.25	8.96	8.00	20.67	13.62

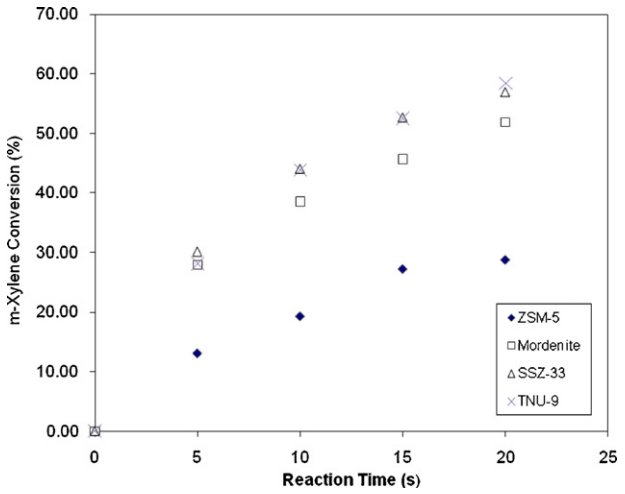

Fig. 3. Xylene conversions versus contact time at 300 °C over 4 zeolites.

why disproportionation products toluene and TMB in Tables 2–5 are much higher in Mordenite, SSZ-33 and TNU-9 compared to ZSM-5 zeolite that is generally considered to favor the unimolecular isomerization pathway.

4.2. *m*-Xylene reactivity over the different zeolite catalysts

Conversions of *m*-xylene reactions over the 4 studied zeolite catalysts are plotted against reaction time in Figs. 3 and 4 at 300 °C and 400 °C. At 300 °C and reaction time of 20 s, Fig. 3 shows that *m*-xylene conversion reached a conversion of 28.87% over ZSM-5, compared to 51.89%, 56.89% and 58.43% over the remaining 3 zeolites; mordenite, SSZ-33 and TNU-9 respectively. Similarly, at 400 °C and reaction time of 20 s, Fig. 4 shows that *m*-xylene conversion reached a conversion of 43.7% over ZSM-5, compared to about 63% over the remaining 3 zeolites at the same condition. It is clear from these Figs. 3 and 4 and Tables 2–5 that the reactivity of *m*-xylene is approximately same over mordenite, SSZ-33 and TNU in the temperature range between 350 °C and 400 °C. Furthermore, with the significant increase in *m*-xylene conversion from 300 °C to 400 °C over ZSM-5, it shows *m*-xylene conversion has not reached its optimum value as higher reaction temperatures may lead to much higher conversions as compared to the remaining 3 zeolites where *m*-xylene conversion is approaching a plateau at approximately 63%.

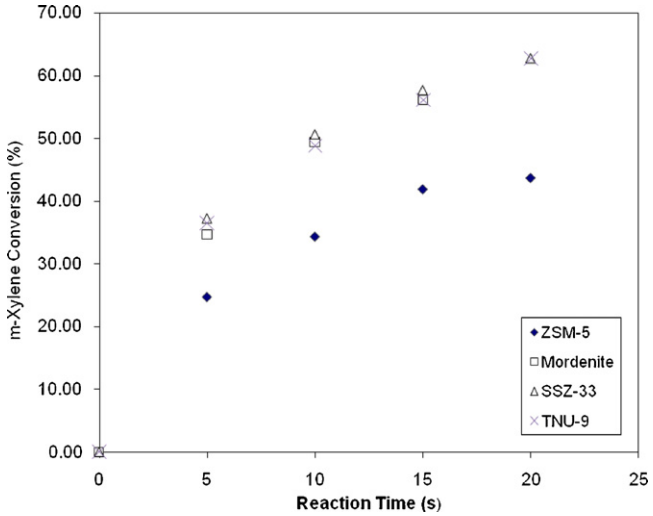

Fig. 4. Xylene conversions versus contact time at 400 °C over 4 zeolites.

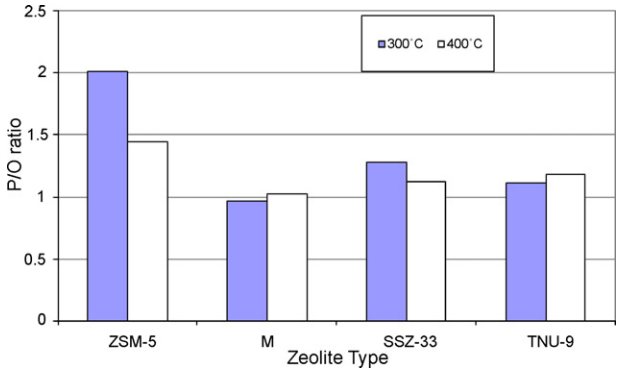

Fig. 5. P/O ratio over 4 zeolite catalysts at 300 and 400 °C.

The reactivity of *m*-xylene over the 12-12-10-ring SSZ-33 catalyst can be attributed to high acidity of this zeolite together with its combined large and medium pore channels allowing increased reaction rate and faster diffusion of both reactants and products. Similarly, high acidity of TNU-9 may account for its high *m*-xylene reactivity. Mordenite took advantage of its pore size to deliver higher *m*-xylene reactivity despite its lower total acidic sites. Therefore, *m*-xylene reactivity in its isomerization and disproportionation reactions over the different zeolite catalysts follows the order: mordenite ≈ SSZ-33 ≈ TNU-9 > ZSM-5.

4.3. *p*-Xylene to *o*-xylene (P/O) ratio

The ratios of *para*- to *ortho*-xylene (P/O) in the product mixture are presented in Fig. 5 at both 300 °C and 400 °C. ZSM-5, a *p*-xylene selective zeolite is shown to have a P/O ratio that is much greater than the equilibrium value of 1.0. ZSM-5 posted a P/O ratio of 2.0 at 300 °C that decreases to 1.45 at 400 °C. The high P/O ratio is due to the high diffusivity of *p*-xylene that is approximately 100 times higher than *o*-xylene as reported by Mirth et al. [26], that enables it leave ZSM-5 structure as soon it forms. Collins et al. [3] obtained 1.35 P/O ratio at 300 °C, while Mirth et al. [26] reported a P/O ratio of around 2.0 at a temperature range of 250–300 °C. Our current value is more in line with Mirth et al. [26] reported value.

The P/O ratio over mordenite is approximately 1.0, the equilibrium value. The ratio over SSZ-33 decreased from 1.28 at 300 °C to 1.12 at 400 °C. TNU-9 behaving like the 10-ring ZSM-5 had a P/O ratio of approximately 1.18 over the 300–400 °C temperature range. The decrease of P/O ratio with temperature could be attributed to the great influence of temperature on the configurational diffusion of *o*-xylene. At 400 °C, *m*-xylene P/O ratio over the different zeolite catalysts was found to be in the following order: ZSM-5 > TNU-9 > SSZ-33 > mordenite.

4.4. Isomerization to disproportionation (I/D) ratio

ZSM-5 consistently gave higher isomerization yields compared disproportionation as shown in Fig. 6. Figure shows isomerization to disproportionation (I/D) ratios decreasing from 3.81 to 2.12 over ZSM-5 at temperature range of 300–400 °C. The I/D ratios over SSZ-33, Mordenite and TNU-9 are low ranging between 0.4 and 0.6. These results indicate ZSM-5 zeolite generally favors the unimolecular isomerization pathway, while disproportionation reaction that requires two molecules of xylene reactants with bulky transition state intermediates is favored by medium and large pore zeolites such as mordenite and SSZ-33 that can accommodate these intermediates. Isomerization and disproportionation pathways have equal possibilities over TNU-9 with its I/D ratio of approximately 0.5. It can be observed from Fig. 6 that at 400 °C, *m*-xylene I/D

Fig. 6. Isomerization to disproportionation products ratio over 4 zeolite catalysts at 300 and 400 °C.

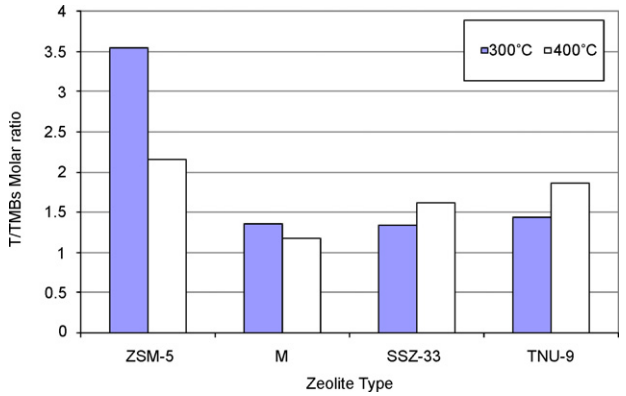

Fig. 7. Toluene to trimethylbenzenes molar ratio over 4 zeolite catalysts at 300 °C and 400 °C.

ratio in its isomerization and disproportionation reactions over the different zeolite catalysts follows the order: ZSM-5 > TNU-9 > SSZ-33 > mordenite.

4.5. Toluene to trimethylbenzenes molar ratio

Fig. 7 shows toluene-to-trimethylbenzenes (T/TMBs) ratios over the various zeolite catalysts. In the absence of secondary transalkylation or dealkylation, the molar ratio of T/TMBs should be unity. However, it can be seen in figure that the T/TMBs ratio is higher than the stoichiometric ratio of 1.0. The ratio ranges from 2.2 to 3.55 over ZSM-5, around 1.2–1.4 over mordenite, 1.3–1.6 over SSZ-33 and 1.4–1.9 over TNU-9. The higher ratio of T/TMBs indicates that either secondary transalkylation or dealkylation reactions are taking place. The dealkylation reaction was found to be inconsequential due to the very small amount of gases observed. TMBs may then have been trapped in micro pores as coke precursors to account for the excess toluene in relation to TMBs, or it may be attributed to the higher desorption rates of toluene as compared to trimethylbenzenes. In conclusion, the results in Fig. 7 show that *m*-xylene T/TMBs ratio in its isomerization and disproportionation reactions over the different zeolite catalysts follows the order: ZSM-5 > TNU-9 > SSZ-33 > mordenite.

Table 6
Apparent kinetic parameters based on time on stream (TOS model)—*m*-xylene isomerization and disproportionation reactions over ZSM-5.

Parameters	Values		
	k_1	k_2	k_4
E_i (kJ/mol)	9.96	21.67	33.45
95% CL	3.59	6.32	7.91
k_{0i}[a] $\times 10^3$ (m^3/kg of catalyst s)	1.22	0.69	0.02
95% CL $\times 10^3$	0.05	0.001	0.002

$\alpha = 0.08$ (95% CL of 0.02).

[a] Pre-exponential factor as obtained from Eq. (5); unit for second order (m^6/kg of catalyst s).

4.6. Discussion of kinetic modeling results

The intrinsic kinetic parameters k_{0i}, E_i, and α, for the *m*-xylene isomerization and disproportionation reactions taking place over the various zeolite catalysts are reported in Tables 6, 8, 10 and 12 with their corresponding 95% confidence limits (CL). They were obtained using non-linear regression (MATLAB package) using the catalyst activity decay function based on time-on-stream (TOS) as described in section 3. The correlation matrices presented in Tables 7, 9, 11 and 13 displayed low cross-correlation between the regressed parameters indicating accurate fit.

It can be observed in Table 6, that *m*-xylene disproportionation reaction over ZSM-5 has the highest apparent activation energy, E_4 with a value of 33.45 kJ/mol. The results in Table 6 also reveal that conversion to *p*-xylene was the easiest with activation energy of 9.96 kJ/mol. The conversion to *o*-xylene was found to have an activation energy of 21.67 kJ/mol. The results explain the high value of I/D ratio posted by ZSM-5 as discussed in Section 4.4 since the isomerization pathway is much easier over ZSM-5.

Yeong et al. [27] recently reported activation energies of 14.3 and 23.49 kJ/mol for *m*-xylene conversion to *p*-xylene and *o*-xylene, respectively over MAFS-A10 (arenesulfonic acid-functionalized silicalite-1 membrane). It can be observed that activation energies obtained in the present study are slightly lower than those reported by Yeong et al. [27] but very consistent with our earlier reported values [2]. Furthermore, it can be seen from Table 6 that catalyst deactivation was found to be small, $\alpha = 0.08$, indicating low coke. It is observed from Table 6 that the order of ease in *m*-xylene isomerization and disproportionation reactions is in the order: $E_4 > E_2 > E_1$. (E_1, E_2 and E_4 are the apparent activation energies of for *m*-xylene isomerization to *p*-xylene, isomerization to *o*-xylene and disproportionation to toluene and TMBs respectively, as given in Scheme 1).

Table 8 reports the parameters obtained over mordenite under similar conditions. From the results, it can be seen that catalyst deactivation was also small, $\alpha = 0.05$. Apparent activation energies of 8.11, 10.64 and 13.94 kJ/mol were obtained for *m*-xylene

Table 7
Correlation matrix for parameters over ZSM-5.

	k_{01}	E_1	k_{02}	E_2	k_{04}	E_4	α
k_{01}	1.000	−0.048	0.575	0.004	0.359	0.056	0.864
E_1	−0.048	1.000	0.008	−0.115	0.095	−0.370	−0.021
k_{02}	0.575	0.008	1.000	−0.248	0.182	0.131	0.709
E_2	0.004	−0.115	−0.248	1.0000	0.153	−0.417	−0.013
k_{04}	0.359	0.095	0.182	0.153	1.000	−0.413	0.594
E_4	0.056	−0.370	0.131	−0.417	−0.413	1.0000	−0.015
α	0.864	−0.021	0.709	−0.013	0.594	−0.015	1.0000

Table 8
Apparent kinetic parameters based on time on stream (TOS model)—*m*-xylene isomerization and disproportionation reactions over mordenite.

Parameters	Values		
	k_1	k_2	k_4
E_i (kJ/mol)	8.11	10.64	13.94
95% CL	7.51	7.72	3.00
k_{0i}[a] × 10^3 (m^3/kg of catalyst s)	0.66	0.64	0.06
95% CL × 10^3	0.08	0.08	0.005

α = 0.05(95% CL of 0.01).
[a] Pre-exponential factor as obtained from Eq. (5); unit for second order (m^6/kg of catalyst s).

Table 9
Correlation matrix for parameters over mordenite.

	k_{01}	E_1	k_{02}	E_2	k_{04}	E_4	α
k_{01}	1.000	−0.031	0.308	0.001	0.430	0.006	0.619
E_1	−0.031	1.000	0.001	−0.113	0.008	−0.288	−0.013
k_{02}	0.308	0.001	1.000	−0.079	0.421	0.015	0.610
E_2	0.001	−0.113	−0.079	1.0000	0.013	−0.289	−0.013
k_{04}	0.430	0.008	0.421	0.013	1.000	−0.056	0.871
E_4	0.006	−0.288	0.015	−0.289	−0.056	1.0000	−0.040
α	0.619	−0.013	0.610	−0.013	0.871	−0.040	1.0000

Table 10
Apparent kinetic parameters based on time on stream (TOS model)—*m*-xylene isomerization and disproportionation reactions over SSZ-33.

Parameters	Values		
	k_1	k_2	k_4
E_i (kJ/mol)	4.58	7.05	8.56
95% CL	3.57	4.20	1.45
k_{0i}[a] × 10^3 (m^3/kg of catalyst s)	0.73	0.62	0.07
95% CL × 10^3	0.04	0.04	0.003

α = 0.05 (95% CL of 0.006).
[a] Pre-exponential factor as obtained from Eq. (5); unit for second order (m^6/kg of catalyst s).

isomerization to *p*-xylene, isomerization to *o*-xylene and disproportionation to toluene and TMBs, respectively. The results indicate that the order of ease in *m*-xylene isomerization and disproportionation reactions over mordenite follows the order: $E_4 > E_2 > E_1$ (Table 8).

The results given in Table 10 are for the reactions over SSZ-33. Similarly, apparent activation energies of 4.58, 7.05 and 8.56 kJ/mol were obtained for *m*-xylene isomerization to *p*-xylene, isomerization to *o*-xylene and disproportionation to toluene and TMBs, respectively. The results show much lower activation energies compared to either ZSM-5 or mordenite, which can be attributed to its high acidity and increased mass transport through its large and medium pore channels. The order of ease in *m*-xylene isomerization and disproportionation reactions over SSZ-33 was also found to be as follows: $E_4 > E_2 > E_1$ (Table 10).

The results given in Table 12 for TNU-9 also show similar trend to ZSM-5 results. The apparent activation energies of 12.11, 13.65 and

Table 11
Correlation matrix for parameters over SSZ-33.

	k_{01}	E_1	k_{02}	E_2	k_{04}	E_4	α
k_{01}	1.000	0.012	0.294	−0.003	0.458	−0.006	0.633
E_1	0.012	1.000	−0.002	−0.110	−0.001	−0.257	−0.009
k_{02}	0.294	−0.002	1.000	−0.036	0.397	0.004	0.575
E_2	−0.003	0.110	−0.036	1.0000	0.004	−0.269	−0.009
k_{04}	0.458	−0.001	0.397	0.004	1.000	−0.017	0.874
E_4	−0.006	−0.257	0.004	−0.269	−0.017	1.0000	−0.027
α	0.633	−0.009	0.575	−0.009	0.874	−0.027	1.0000

Table 12
Apparent kinetic parameters based on time on stream (TOS model)—*m*-xylene isomerization and disproportionation reactions over TNU-9.

Parameters	Values		
	k_1	k_2	k_4
E_i (kJ/mol)	12.11	13.65	24.99
95% CL	8.22	10.10	4.47
k_{0i}[a] × 10^3 (m^3/kg of catalyst s)	0.70	0.60	0.06
95% CL × 10^3	0.21	0.20	0.01

α = 0.02 (95% CL of 0.02).
[a] Pre-exponential factor as obtained from Eq. (5); unit for second order (m^6/kg of catalyst s).

24.99 kJ/mol were obtained for *m*-xylene isomerization to *p*-xylene, isomerization to *o*-xylene and disproportionation to toluene and TMBs, respectively. In addition, the results show much lower activation energies for *o*-xylene isomerization and disproportionation reactions compared to ZSM-5, but higher activation energy for *p*-xylene isomerization. It is therefore expected to have more disproportionation products over TNU-9 as compared to ZSM-5 as evidenced from the lower TNU-9 activation energy of 24.99 kJ/mol for disproportionation compared to 33.45 kJ/mol for ZSM-5. The slightly larger pores of TNU-9 than ZSM-5 could explain the differences in the results. The order of ease in *m*-xylene isomerization and disproportionation reactions over TNU-9 was found to be in the order: $E_4 > E_2 > E_1$ (Table 12).

In order to compare the overall performance of the four studied zeolite catalysts, their various activation energies for isomerization and disproportionation are plotted in Fig. 8. It is observed from the figure that the activation energy for the *m*-xylene disproportionation reaction was found to increase in the order: SSZ-33 (8.56 kJ/mol) < mordenite (13.94 kJ/mol) < TNU-9 (24.99 kJ/mol) < ZSM-5 (33.45 kJ/mol). Furthermore, the figure shows that isomerization to *p*-xylene activation energy was found to decrease in the order: TNU-9 (12.11 kJ/mol) > ZSM-5 (9.96 kJ/mol) > mordenite (8.11 kJ/mol) > SSZ-33 (4.58 kJ/mol), while the activation energy for isomerization to *o*-xylene decreases from ZSM-5 (21.67 kJ/mol) > TNU-9 (13.65 kJ/mol) > mordenite (10.64 kJ/mol) > SSZ-33 (7.05 kJ/mol).

The comparisons between experimental and predicted product distributions over the various zeolites are shown at 400 °C in Figs. 9–12. It can be observed that the predicted results are in good agreement with the experimental results within an error of less than ±5%. These results indicate that 1,2-methyl shift reaction scheme based on time on stream (TOS) models (Eqs. (1)–(7)) is appropriate for *m*-xylene isomerization and disproportionation reactions over zeolite catalysts in a riser simulator.

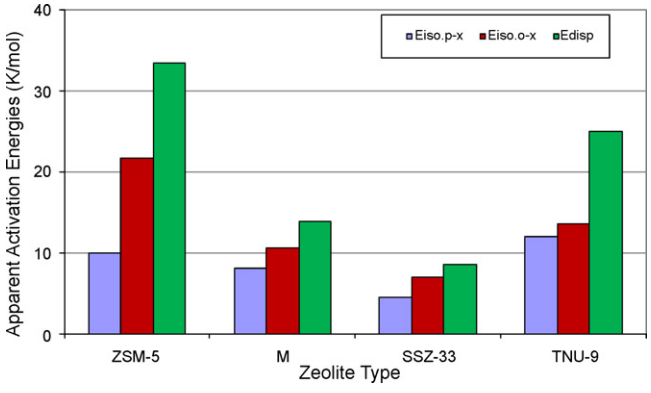

Fig. 8. Comparison of apparent activation energies over the 4 zeolite catalysts.

Table 13
Correlation matrix for parameters over TNU-9.

	k_{01}	E_1	k_{02}	E_2	k_{04}	E_4	α
k_{01}	1.000	0.609	0.146	−0.086	0.240	−0.194	0.509
E_1	0.609	1.000	−0.093	−0.126	−0.161	−0.322	−0.035
k_{02}	0.146	−0.093	1.000	0.622	0.185	−0.204	0.453
E_2	−0.086	−0.126	0.622	1.0000	−0.159	−0.335	−0.028
k_{04}	0.240	−0.161	0.185	−0.159	1.000	0.383	0.745
E_4	−0.194	−0.322	−0.204	−0.335	0.383	1.0000	−0.099
α	0.509	−0.035	0.453	−0.028	0.745	−0.099	1.0000

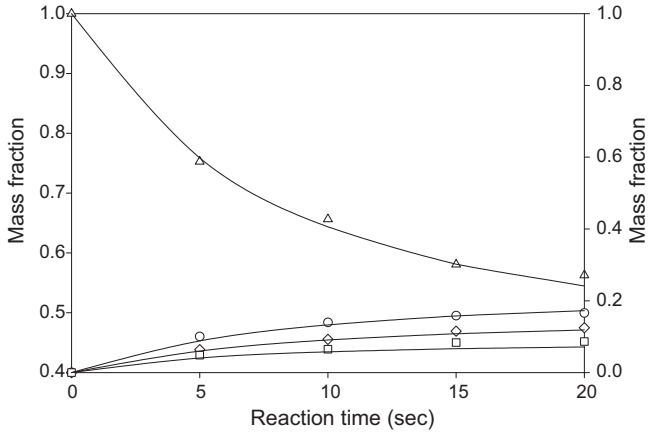

Fig. 9. Comparison between experimental and predicted product distributions over ZSM-5 at 400 °C [△ = *m*-xylene; ◯ = *p*-xylene; ◊ = o-xylene; □ = toluene].

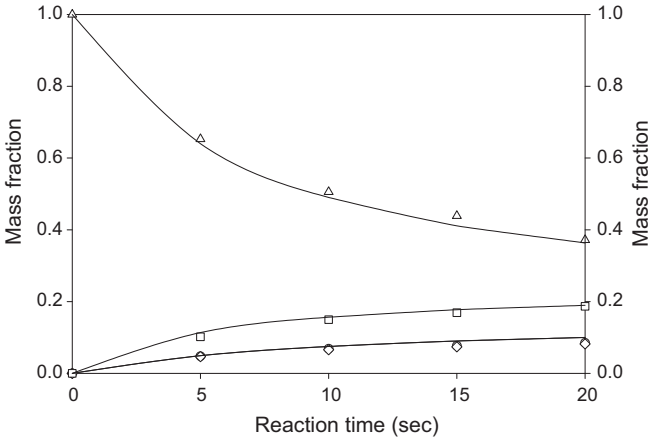

Fig. 10. Comparison between experimental and predicted product distributions over mordenite at 400 °C [△ = *m*-xylene; ◯ = *p*-xylene; ◊ = o-xylene; □ = toluene].

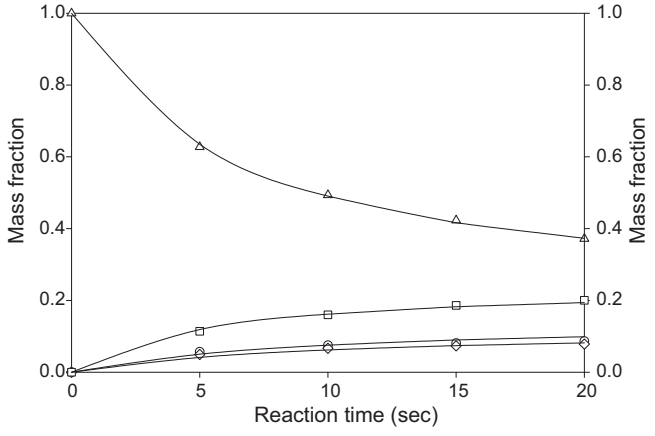

Fig. 11. Comparison between experimental and predicted product distributions over SSZ-33 at 400 °C [△ = *m*-xylene; ◯ = *p*-xylene; ◊ = o-xylene; □ = toluene].

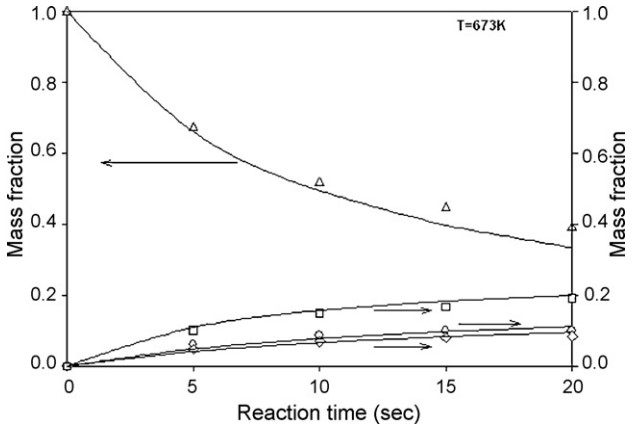

Fig. 12. Comparison between experimental and predicted product distributions over TNU-9 at 400 °C [△ = *m*-xylene; ◯ = *p*-xylene; ◊ = o-xylene; □ = toluene].

5. Conclusions

The following conclusions can be drawn from *m*-xylene isomerization and disproportionation reactions over zeolite catalysts:

1. The experimental results show that SSZ-33, TNU-9 and mordenite performed better in *m*-xylene isomerization and disproportionation reactions as compared to ZSM-5, with *m*-xylene conversion of approximately 63% at 400 °C and reaction time of 20 s. *m*-Xylene reactivity was found to be in the following order: mordenite ≈ SSZ-33 ≈ TNU-9 > ZSM-5.
2. ZSM-5 posted a P/O ratio of at least 1.45 greater than the equilibrium value due to the high diffusivity of *p*-xylene that enables it leave ZSM-5 structure as soon it forms. P/O ratio resulting from *m*-xylene conversion over the different zeolite catalysts was found to be in the following order: ZSM-5 > TNU-9 > SSZ-33 > mordenite.
3. The results show that ZSM-5 consistently gave higher isomerization yields compared to disproportionation. Isomerization to disproportionation reactions ratio (I/D) over the different zeolite catalysts follows the order: ZSM-5 > TNU-9 > SSZ-33 > mordenite.
4. Kinetic parameters for *m*-xylene isomerization and disproportionation reactions have been determined using catalyst activity decay function based on time on stream (TOS). Over each zeolite, the order of ease for the *m*-xylene isomerization and disproportionation reaction was found to be in the order: $E_4 > E_2 > E_1$. Comparing the overall performance of the zeolites, apparent activation energy for *m*-xylene disproportionation reaction was found to decrease in the order: $E_{ZSM\text{-}5} > E_{TNU\text{-}9} > E_{mordenite} > E_{SSZ\text{-}33}$; activation energy for isomerization to *p*-xylene decreases in the order: $E_{TNU\text{-}9} > E_{ZSM\text{-}5} > E_{mordenite} > E_{SSZ\text{-}33}$; while activation energy for isomerization to *o*-xylene decreases from $E_{ZSM\text{-}5} > E_{TNU\text{-}9} > E_{mordenite} > E_{SSZ\text{-}33}$.
5. The riser simulator and the modeling procedures employed have shown to be very effective in investigating xylene kinetics.

Acknowledgments

The authors acknowledge the support from Ministry of Higher Education, Saudi Arabia for the establishment of the Center of Research Excellence in Petroleum Refining and Petrochemicals at King Fahd University of Petroleum and Minerals (KFUPM). The authors thank J. Heyrovsky Institute of Physical Chemistry for providing zeolites TNU-9 and SSZ-33 and their characterization.

References

[1] J. Čejka, B. Wichterlová, Acid-catalyzed synthesis of mono- and dialkyl benzenes over zeolites: active sites, zeolite topology, and reaction mechanisms, Catal. Rev. 44 (2002) 375–421.
[2] S. Al-Khattaf, N.M. Tukur, A. Al-Amer, Modeling xylene reactions over ZSM-5 zeolite in a riser simulator: 1,3 versus 1,2-methyl shift, Ind. Eng. Chem. Res. 44 (2005) 7957–7968.
[3] D.J. Collins, R.J. Medina, B.H. Davis, Xylene isomerization by ZSM-5 zeolite catalyst, Can. J. Chem. Eng. 61 (1983) 29.
[4] Y.S. Hsu, T.Y. Lee, H.C. Hu, Isomerization of ethylbenzene and m-xylene on zeolites, Ind. Eng. Chem. Res. 27 (1988) 942.
[5] X. Chang, Y. Li, Z. Zeng, Kinetics study of the isomerization of xylene on HZSM-5 zeolite. 1. Kinetics model and reaction mechanism, Ind. Eng. Chem. Res. 31 (1992) 187.
[6] L.B. Young, S.A. Butter, W.W. Kaeding, Shape selective reactions with zeolite catalysts: III. Selectivity in xylene isomerization, toluene–methanol alkylation, and toluene disproportionation over ZSM-5 zeolite catalysts, J. Catal. 76 (1982) 418.
[7] M.A. Lanewola, A.P. Bolton, Isomerization of the xylenes using zeolite catalysts, J. Org. Chem. 34 (1969) 3107.
[8] P. Chutoransky, F.G. Dwyer, Effect of zeolite crystallite size on the selectivity kinetics of the heterogeneous catalyzed isomerization of xylenes, Adv. Chem. Ser. 121 (1974) 540.
[9] D.J. Collins, K.J. Mulrooney, R.J. Medina, B.H. Davis, Xylene isomerization and disproportionation over lanthanum Y catalyst, J. Catal. 75 (1982) 291.
[10] A. Cortes, A. Corma, The mechanism of catalytic isomerization of xylenes: kinetic and isotopic studies, J. Catal. 51 (1978) 338.
[11] T. Tsai, S. Liu, I.I. Wang, Disproportionation and transalkylation of alkylbenzenes over zeolite catalysts, Appl. Catal. A: Gen. 181 (1999) 355–398.
[12] Y.H. Ma, L.A. Savage, Xylene isomerization using zeolites in a gradientless reactor system, AIChE J. 33 (1987) 1233–1240.
[13] A. Iliyas, S. Al-Khattaf, Xylene isomerization over USY zeolite in a riser simulator: a comprehensive kinetic model, Ind. Eng. Chem. Res. 43 (2004) 1349.
[14] S. Al-Khattaf, Xylenes reactions and diffusions in ZSM-5 zeolite based catalyst, Ind. Eng. Chem. Res. 46 (2007) 59–69.
[15] N. Žilková, M. Bejblová, B. Gil, S.I. Zones, A.W. Burton, C.-Y. Chen, Z. Musilová-Pavlačková, G. Košová, J. Čejka, The role of the zeolite channel architecture and acidity on the activity and selectivity in aromatic transformations: the effect of zeolite cages in SSZ-35 zeolite, J. Catal. 266 (2009) 79–91.
[16] F.J. Llopis, G. Sastre, A. Corma, Xylene isomerization and aromatic alkylation in zeolites NU-87, SSZ-33, β, and ZSM-5: molecular dynamics and catalytic studies, J. Catal. 227 (2004) 227–241.
[17] S. Al-Khattaf, Z. Musilova-Pavlackova, M.A. Ali, J. Cejka, Comparison of activity and selectivity of SSZ-33 based catalyst with other zeolites in toluene disproportionation, Top. Catal. 52 (2009) 140–147.
[18] J. Cejka, N. Zilkova, S.I. Zones, M. Bejblova, Novel zeolites in transformation of aromatic hydrocarbons, in: 18th Saudi Japan Symposium, Dhahran, Saudi Arabia, November, 2008.
[19] C.A. Emeis, Determination of integrated molar extinction coefficients for infrared absorption bands of pyridine adsorbed on solid acid catalysts, J. Catal. 141 (1993) 347–354.
[20] B. Gil, S.I. Zones, S.J. Hwang, M. Bejblova, J. Cejka, Acidic properties of SSZ-33 and SSZ-35 novel zeolites: a complex infrared and MAS NMR study, J. Phys. Chem. C 112 (2008) 2997–3007.
[21] H.T. de Lasa, US Patent 5,102 (1992) 628.
[22] D.W. Kraemer, Modelling Catalytic Cracking in a Novel Riser Simulator, Ph.D. Dissertation, University of Western Ontario, London, Canada, 1991.
[23] J.A. Atias, G. Tonetto, H. de Lasa, Catalytic conversion of 1,2,4-trimethylbenzene in a CREC riser simulator. A heterogeneous model with adsorption and reaction phenomena, Ind. Eng. Chem. Res. 42 (2003) 4162–4173.
[24] T.S. Gendy, Simulation of liquid and vapour phase xylene isomerization over deactivating H-Y-zeolite, J. Chem. Technol. Biotechnol. 73 (1998) 109.
[25] D.R. Stull, E.F. Westrum, G.C. Simke, The Chemical Thermodynamics of Organic Compounds, Wiley, New York, 1969, p. 368.
[26] G. Mirth, J. Cejka, J.A. Lercher, Transport and isomerization of xylenes over HZSM-5 zeolites, J. Catal. 139 (1993) 24–33.
[27] Y.F. Yeong, A.Z. Abdullah, A. Ahmad, S.S. Bhatia, Xylene isomerization kinetic over acid-functionalized silicalite-1 catalytic membranes: experimental and modeling studies, Chem. Eng. J. 157 (2010) 579–589.